Int. J. Heat Mass Transfer. Vol. 30, No. 4, pp. 663–672, 1987
Printed in Great Britain

0017–9310/87 $3.00 + 0.00
Pergamon Journals Ltd.

Fluid flow and heat transfer in incandescent lamps

S. M. CORREA
General Electric Company, Research and Development Center,
P.O. Box 8, Schenectady, NY 12301, U.S.A.

(*Received* 21 *November* 1985 *and in final form* 18 *July* 1986)

Abstract—A numerical model is developed to study the two-dimensional laminar, natural-convection flow in incandescent lamps by a finite-volume solution of the steady continuity, Navier–Stokes and energy equations on a curvilinear body-fitted computational grid. The model is applied to typical vertically- and horizontally-oriented lamps containing an inert gas at high pressure. The predicted heat transfer from the filament agrees to within 15% with a semi-empirical correlation. The relationship of the flowfield to observed blackening patterns is discussed. Transport of minor species is formulated and computed for inert tungsten vapor.

1. INTRODUCTION

SIGNIFICANT improvements in the life and efficiency of incandescent lamps can follow from a detailed knowledge of the physico-chemical processes involved. The flow and temperature fields and the distribution of chemical species are of particular importance. These lamps are filled with an inert gas to inhibit the otherwise rapid diffusion of tungsten to the walls and the accompanying loss of light output. The resulting natural-convection flow cools the filament, so reducing efficiency, and transports tungsten and a variety of chemical species in a cyclical path between the filament and the walls. Higher filling pressures enhance the importance of convection over diffusion. Early models of the flow within incandescent lamps hypothesized a thin stagnant conduction-dominated layer surrounding the filament, within which the transition from filament to wall temperature occurred [1,2]. These models provided reasonable estimates of gross heat transfer but are insensitive to orientation and geometry and cannot account for flow outside the filament boundary layer. To obtain the complete flowfield, Navier–Stokes equations with buoyancy must be solved; due to their nonlinearities and the complex geometries of interest, analytical closed-form solutions are not available. The purpose of this paper is to formulate a computational model for the flow, heat and mass transport within incandescent lamps and to demonstrate it for typical cases.

Incandescent *halogen* lamps are characterized by the addition of trace quantities of additives such as methyl bromide, which dissociate and chemically fix wall deposits as gaseous chemical species. These are transported back to the filament where the tungsten is liberated by thermal decomposition. This chemistry is crucial to the extension of lamp life via choice of additives but, because it occurs between very dilute species, it does not affect the velocity and temperature fields. Thus the principal hydrodynamic equations decouple from those of the minor species and may be solved first, as described below.

Halogen chemistry in incandescent lamps is the subject of a companion study; for reference, the transport equation for the chemically *inert* flow of tungsten vapor is included here. Thus the present study is pertinent to incandescent non-halogen lamps and provides the basis for halogen lamp models to follow.

While simplified one-dimensional analyses of lamp flows including chemistry have been advanced (e.g. by Harvey [3]), this is one of the first studies of the full elliptic equations governing flow in high-pressure lamps. It therefore makes sense to study the two-dimensional problem because it is quite representative of the flow in lamps, except, for example, at the ends of horizontal lamps or around filament-support structures. Such regions are not expected to significantly affect the overall flow patterns and can be included in later three-dimensional computations, if necessary.

The transient problem of lamp startup is also potentially of interest, particularly as far as the chemistry of the filament material and gaseous additives is concerned. Sell *et al.* [4] have performed spectroscopic analyses of lamps after various lengths of operation, showing that the time required before the reacting gases attain steady-state concentrations can be of the order of minutes. In general, however, even less experimental data is available for the transient flow than for the steady-state flow. Therefore, although the transient flow problem is computationally tractable, to study it at length would be premature.

Steady-state flow in a lamp falls into the category of (low Rayleigh number) natural convection in enclosed

NOMENCLATURE

a,b	numerical coefficients
b	sheath diameter
d	filament diameter
D	diffusion coefficient
f	functional form
Gr	Grashof number
h	height
H	enthalpy
J	Jacobian
Nu	Nusselt number
Pr	Prandtl number
q_1, q_2, q_3	products of metric coefficients
Q	heat transfer
r	radial coordinate
Ra	Rayleigh number
S	source term
T	temperature
t	sheath thickness
u	axial velocity
U	contravariant velocity component
v	radial velocity
V	contravariant velocity component
W	total kinetic energy
x	axial coordinate
y	transverse coordinate
Y	mass fraction.

Greek symbols

Γ	transport coefficient
η	generalized coordinate
θ	non-dimensional temperature
λ	thermal conductivity
ξ	generalized coordinate
ρ	density
ϕ	generalized variable.

Subscripts

f	filament
T	thermal diffusion
w	wall, tungsten
ξ	differentiation with respect to ξ
η	differentiation with respect to η.

cavities. Such flows are of significance in a variety of technological devices, ranging from nuclear power plants to space-based material processors. In modified form these flows have also received attention as 'benchmark' test cases for numerical methods. De Vahl Davis and Jones [5] reviewed numerical solutions contributed by about 40 independent groups using several different techniques. The test problem was the flow in a planar square cavity with facing hot and cold side walls and adiabatic top and bottom walls. The Prandtl number was prescribed as 0.71. About one-half of the contributions used finite-difference methods and about one-quarter used finite-element methods. A conclusion relevant to the present study is that for Rayleigh numbers as low as in a typical lamp ($\sim 10^2 - 10^3$), most finite-difference numerical methods are adequate. It should also be noted that the flow remains laminar in this range, so that turbulence models with their attendant errors are not required.

Because incandescent lamps are operated either vertically or horizontally, two different idealized geometries are considered. In the vertical case, the computational domain is axisymmetric with a filament at the center-line, extending from just above the bottom to just below the top of the lamp: the gaps are taken as being approximately 3% of the height of the lamp. In the horizontal case, the planar domain corresponds to a vertical cross-section of the lamp with the filament at the center. Each case has special features as discussed below.

2. FORMULATION OF MODEL

The continuity, Navier–Stokes and energy equations may be cast in a common form. For steady, axisymmetric, two-dimensional flow, the general equation for the dependent variable ϕ is

$$\frac{1}{r}\left[\frac{\partial}{\partial x}(\rho u r\phi) + \frac{\partial}{\partial r}(\rho v r\phi)\right] = \frac{1}{r}\left[\frac{\partial}{\partial x}\left(r\Gamma\frac{\partial\phi}{\partial x}\right) + \frac{\partial}{\partial r}\left(r\Gamma\frac{\partial\phi}{\partial r}\right)\right] + S \qquad (1)$$

where $\phi = 1, u, v$, and H, in turn for the four equations of interest, Γ is correspondingly zero, the viscosity or the thermal diffusivity (to within a factor of density) and the source term S represents the pressure gradient and buoyancy terms in the Navier–Stokes equations and is zero in the others. Viscosity and thermal conductivity of the inert gas are available as explicit functions of temperature.

It should be noted that *free* natural convection flows are of the boundary-layer type being governed by the parabolic form of equation (1). However, this is not the case here because the flow occurs in an *enclosed* cavity. The governing equations thus remain elliptic and boundary-layer analysis such as that due to Sparrow and Gregg [6] is not applicable.

Tungsten transport in the case of no chemical reactions is governed by equation (1) with ϕ being the concentration of tungsten and the source term S including the flux due to thermal diffusion. The

diffusion coefficients are available as functions of temperature. Again, since the vapour pressure of tungsten in these systems is very small, the equation is decoupled from the principal hydrodynamic set. Thus the velocity and temperature fields are computed separately at first. The tungsten transport equation is then nonlinear only because of the dependence of the thermal diffusion coefficient on concentration.

With the introduction of new independent variables ξ and η, equation (1) changes according to the general transformation $\xi = \xi(x,r), \eta = \eta(x,r)$. Equation (1) may be rewritten in (ξ,η) coordinates as [7]

$$\frac{1}{rJ}\left[\frac{\partial}{\partial\xi}(\rho U r\phi) + \frac{\partial}{\partial\eta}(\rho V r\phi)\right] = \frac{1}{rJ}\frac{\partial}{\partial\xi}\left[\frac{\Gamma}{J}(q_1 r\phi_\xi - q_2 r\phi_\eta)\right] + \frac{1}{rJ}\frac{\partial}{\partial\eta}\left[\frac{\Gamma}{J}(-q_2 r\phi_\xi + q_3 r\phi_\eta)\right] + S(\xi,\eta) \quad (2a)$$

where

$$U = ur_\eta - vx_\eta \quad (2b)$$

$$V = vx_\xi - ur_\xi \quad (2c)$$

$$q_1 = x_\eta^2 + r_\eta^2 \quad (2d)$$

$$q_2 = x_\xi x_\eta + r_\xi r_\eta \quad (2e)$$

$$q_3 = x_\xi^2 + r_\xi^2 \quad (2f)$$

$$J = x_\xi r_\eta - x_\eta r_\xi \quad (2g)$$

and $S(\xi,\eta)$ is the source term of the governing equation in (ξ,η) coordinates. This numerical coordinate transformation results in a regular domain in the computational plane regardless of the complexity of the original domain.

Boundary conditions for the hydrodynamic equations are obtained from no-slip and prescribed temperature conditions. In the vertical case (Fig. 1), along the filament and the walls

$$u = 0, v = 0 \quad (3)$$

and

$$T = T_f \text{ along the filament } r = r_f \quad (4a)$$

$$T = T_w \text{ elsewhere along the boundary.} \quad (4b)$$

By symmetry in the horizontal case (Fig. 2), the computational domain is bounded by a symmetry plane and the lamp wall. The boundary conditions are

$$u = 0,\ v = 0,\ T = T_w \text{ along the wall} \quad (5a)$$

$$u = 0,\ v = 0,\ T = T_f \text{ at the filament} \quad (5b)$$

and

$$\frac{\partial\phi}{\partial y} = 0, \phi = u,v,T \text{ at the symmetry plane.} \quad (5c)$$

Boundary conditions for the tungsten transport equation are obtained by assuming the vapor to be in a saturated state at the filament and the walls. If the mean flux of tungsten at any location along the wall is *into* the lamp, this boundary condition is replaced by a zero-flux boundary condition; the rationale for this is that the wall cannot act as a steady-state source of tungsten.

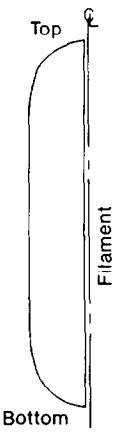

FIG. 1. Vertical lamp.

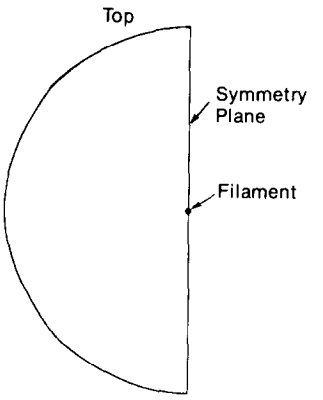

FIG. 2. Horizontal lamp.

The equations are discretized in finite volume form using second-order accurate central differences for the diffusion terms and first- or second-order upwind differencing for the convection terms. In the case of first-order upwind differencing, truncation error introduces an artificial viscosity that is numerically stabilizing but inaccurate. The situation is partially remedied by using second-order central differencing for the convection terms when the grid is fine enough (local cell Peclet/Reynolds number less than two); on coarser grids second-order central differences for convection lead to instability. Further details of the implementation of these finite-difference schemes may be found in Shyy and Correa [7]. Because typical Reynolds numbers in lamp flows are relatively low, inaccuracies introduced by discretization are not significant. The equations are solved in an iterative

sequence similar to the SIMPLE algorithm of Patankar and Spalding [8].

The solution procedure is as follows: the momentum equations are first solved to obtain the velocity components with the given pressure field. When solving the momentum equations, U and V are calculated after updating the velocity field. All the finite-difference equations are solved by the successive line underrelaxation method. After completing a sweep of the entire solution domain, adjustments are made to the pressure field to ensure that continuity is satisfied along every line of cells. Such adjustments destroy the compliance of the velocity and pressure fields with the momentum equations, and, therefore, further iterations are needed until the momentum and continuity equations are simultaneously satisfied.

For the chemically reacting system found in incandescent halogen lamps additional transport equations of similar form would be present. The dependent variables could be elemental activities or concentrations, from the field values of which (equilibrium) species concentrations could be immediately obtained. Thus, for equilibrium flow the number of additional transport equations is the number of elements rather than the number of species. If equilibrium does not prevail, the difficult task of determining chemical kinetic reactions and rates would have to be undertaken. This set of mutually coupled equations for the minor species would still be decoupled from the hydrodynamic set and so would be solved after the flow and temperature fields were obtained.

Simple boundary conditions are employed here for convenience. In reality, the top of a lamp would stabilize at a somewhat higher temperature than the bottom because of the upward convection of hot gas. A more realistic wall boundary condition could be obtained by matching the heat flux from the internal gas to the heat lost locally to the lamp environment, perhaps using an empirical correlation for the latter. The local wall temperature would then emerge as a result of the simulation. However, because the largest difference in temperatures along the wall is expected to be much less than the difference between filament and wall temperatures, this more elaborate boundary condition should not affect the flow field. On the other hand, wall chemistry may be strongly influenced by small differences in the local temperature.

Convergence of the iterative solution algorithm is based on two alternative criteria. Prior to convergence the algebraic finite-difference equations are not satisfied; the corresponding out-of-balance terms or 'residuals' are reduced in the course of iterations. One convergence criterion is based on the residuals falling below certain levels. Another criterion monitors the mean square velocity at each node, i, j

$$W = \sum_i \sum_j (u_{ij}^2 + v_{ij}^2) \tag{6}$$

and continues iterations until W becomes steady.

The velocity and temperature fields can then be used to compute the heat transfer. In particular, the radial heat transfer from the filament is given by

$$Q = -\left[\lambda \frac{\partial T}{\partial r}\right]_{r=r_f}. \tag{7}$$

3. STAGNANT-LAYER THEORY

Because heat transfer from the filament to the gas dissipates part of the input power and decreases lamp efficiency, it has received considerable attention in the past. Langmuir [2] assumed that heat transfer in the prototypical problem of natural convection around a vertical cylinder occurs solely by conduction through a stagnant layer of gas. Outside this layer or sheath, the flow has the free stream temperature. Elenbaas [1,9] reviewed Langmuir's assumptions and matched the sheath theory for large cylinder diameters to vertical flat plate theory to obtain an expression for the Nusselt number. This expresion is valid for a larger range of $Gr\ Pr$ than the original sheath theory. A similar development from Bergman [10] is presented here.

In brief, the stagnant-layer analysis yields

$$Nu = \frac{2}{\ln(b/d)} = \frac{2}{\ln(1 + 2t/d)} \tag{8}$$

where b is the diameter of the sheath and

$$t = \frac{1}{2}(b - d) \tag{9}$$

is its thickness. As the cylinder diameter becomes large, an expansion of equation (8) yields

$$Nu \to \left(\frac{t}{d}\right)^{-1} + \text{higher-order terms.} \tag{10}$$

This result should match that for a flat plate which may be considered as a cylinder with infinitely large diameter. The heat transfer from a vertical flat plate due to natural convection is given by

$$Nu = f(Ra^{1/4}) \tag{11}$$

where

$$Ra = Gr\ Pr \tag{12}$$

is the Rayleigh number. Equating equations (10) and (11), the sheath thickness is obtained as

$$\frac{t}{d} = 1/f(Ra^{1/4}) \tag{13}$$

where f is an unknown function. Thus, the heat transfer may be expressed as

$$Nu = 2/\ln(1 + 2/f(Ra^{1/4})). \tag{14}$$

The function $f(Ra^{1/4})$ is obtained empirically. McAdams [11] tabulated available data for Nu as a function of Ra over the range $10^{-5} < Gr < 10^8$.

Table 1

Lamp	Vertical	Horizontal
Gas	Krypton	Krypton
Pressure (Torr), cold	600	600
Filament height (mm)	30	–
Filament diameter (mm)	1	–
Lamp height (mm)	30	–
Lamp diameter (mm)	10	10
Filament temperature (K)	2725	2725
Wall temperature (K)	400	400
Power (W)	100	100

FIG. 3. Grid for a vertical lamp.

FIG. 4. Velocity field in a vertical lamp.

Bergman [10] curve-fitted this data to obtain the correlation

$$f = (a + b \ln Gr)Ra^{1/4} \tag{15}$$

where a and b are numerical coefficients. Combining equations (14) and (15) gives the final expression for Nu

$$Nu = 2\Big/\ln\left[1 + \frac{2}{(a+b\ln Gr)Ra^{1/4}}\right]. \tag{16}$$

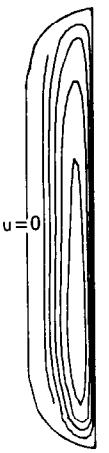

FIG. 5. Axial velocity contours in a vertical lamp ($\Delta u = 0.05\,\mathrm{m\,s^{-1}}$).

Sparrow and Gregg [6] have derived similar expressions for the heat transfer from vertical cylinders in terms of stagnant-layer theory by matching with numerical power series solutions of the free convection boundary layer equations.

4. RESULTS

The numerical model described in Section 2 was applied first to a vertical incandescent lamp as specified in Table 1. The 16 × 16 grid used in the computation is shown in Fig. 3, from which the non-uniform radial distribution and the uniform axial distribution are evident. The results were not substantially changed when denser grids were used because the Reynolds number in the radial direction is small.

The velocity vector field (Fig. 4) and the axial velocity contours (Fig. 5) show a pronounced boundary layer along the filament with the largest velocities being of the order of $0.20\,\mathrm{m\,s^{-1}}$. The return (downward) velocities along the outer wall are substantially lower because of the larger radius there. From the radial velocity contours (Fig. 6) it is clear that except for the end effects at the top and the bottom of the lamp, there is very little radial flow. This is also evident from the isotherms (Fig. 7), which are laterally displaced by the radially outward (inward) velocities at the top (bottom) of the lamp.

Like the isotherms the tungsten mass-fraction contours (Fig. 8) show a predominantly one-dimensional variation except at the top and bottom ends of the lamp. Near the filament, the radial gradient is very steep indicating the presence of a boundary layer. Thermal diffusion is significant in these results and augments the diffusion of tungsten away from the filament. The flux of tungsten is into the wall everywhere along the perimeter.

The net Fick plus thermal diffusion flux of tungsten out of the filament can be determined from the solutions as $(\rho D \nabla Y + \rho D_T Y \nabla T/T)$. Reasonable esti-

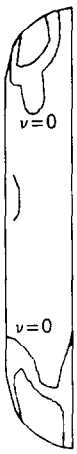

FIG. 6. Radial velocity contours in a vertical lamp ($\Delta v = 0.01 \text{m s}^{-1}$).

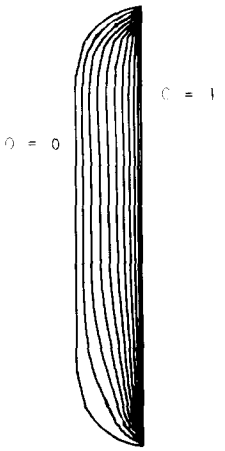

FIG. 7. Contours of non-dimensional temperature θ in a vertical lamp [$\theta = (T - T_{\text{wall}})/(T_{\text{filament}} - T_{\text{wall}})$, $\Delta\theta = 0.1$].

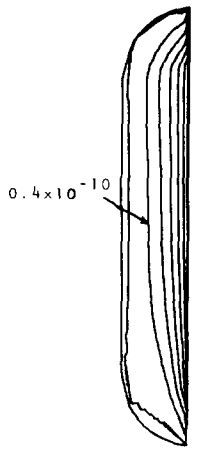

FIG. 8. Tungsten distribution in a vertical lamp, Y_w.

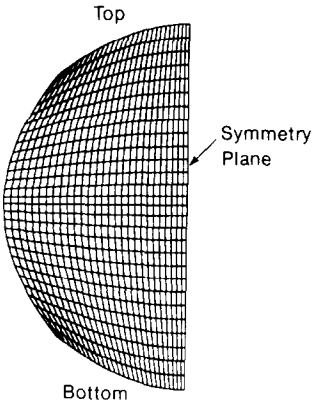

FIG. 9. Grid for a horizontal lamp.

mates of the life of the filament are then obtained by calculating the time for some fraction of the mass of the filament to be lost. Although empiricisms concerning the maximum permissible amount of mass loss due to diffusion are needed, such estimates can help to discriminate between competing lamp designs. This will be particularly interesting when the chemistry of additives found in halogen lamps is included in the model.

The heat transfer from the filament may be computed from the temperature field and equation (7). When the value at the mid-height of the filament is used the heat transfer agrees with the Langmuir sheath value from equation (16) to within 15%. The heat loss of approximately 6 W amounts to 6% of the total electric power into the lamp, and is of the same order as the visible light output. This agreement constitutes a global validation of the accuracy of the numerical model. Measurements of the velocity or temperature fields within the lamp would be required for detailed comparisons.

When adiabatic top and bottom walls are substituted for the isothermal walls at a prescribed temperature, the mid-height heat transfer remains the same. From the bottom to the top of the filament the local heat transfer decreases in agreement with expressions from free natural-convection theory. With isothermal walls, the local heat transfer at the ends of the filament is distorted by the presence of the wall. In an overall sense, therefore, the Langmuir premise of a stagnant region along the filament is corroborated by these computations.

The 29 × 29 computational grid used for the horizontal lamp flow is shown in Fig. 9. The additional grid is needed to adequately resolve the flowfield, particularly in the vicinity of the filament which is taken here to be a point. The distortion of the circular envelope shape to fit the 'box' grid topology is exaggerated. This distortion emphasizes those source terms which originate in the coordinate transformation and can reduce the convergence rate of the algorithm when compared with the vertical lamp. The velocity field and velocity contours for the horizontal

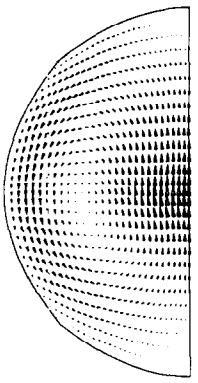

FIG. 10. Velocity field in a horizontal lamp.

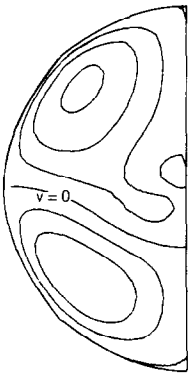

FIG. 12. Horizontal velocity contours in a horizontal lamp ($\Delta v = 0.01\ \mathrm{m\ s^{-1}}$).

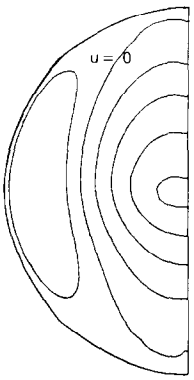

FIG. 11. Vertical velocity contours in a horizontal lamp ($\Delta u = 0.02\ \mathrm{m\ s^{-1}}$).

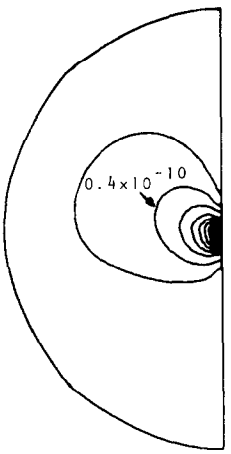

FIG. 13. Tungsten distribution in a horizontal lamp, Y_w.

lamp specified in Table 1 are shown in Figs. 10–12. The flowfield is dominated by a buoyant plume rising from the filament and impinging on the top of the lamp, with a downward return flow along the lamp envelope completing the natural convection cell. Maximum velocities are of the order of $0.10\,\mathrm{m\,s^{-1}}$. Stagnant regions may be seen at the top and the bottom of the lamp, where the flow turns to follow the geometrical constraints imposed by the symmetry plane and the lamp envelope. Within the stagnant regions, secondary flows which rotate in the opposite direction to the primary natural convection cell are possible. Qualitative support for these predictions is available from flow visualization results [12,13].

Mass-fraction contours of tungsten (Fig. 13) are also distorted by the upward flow of gas near the filament. These results indicate that the gradients are steepest at the bottom of the filament where there is a stagnation point. The flow of tungsten is not directly upward but to the sides because of the blockage exerted by the stagnant region, suggesting a preferred direction for blackening of the lamp wall.

The observed blackening patterns in horizontal halogen lamps might be rationalized in terms of the stagnant region as follows. Matter is transported across the streamline which divides the primary and secondary flows by diffusion only. Being lighter than tungsten (molecular weight 184), bromine (80) diffuses into this secondary cell more rapidly. Therefore the region at the top of the lamp should be lean in tungsten and rich in bromine, which expedites the wall-cleaning chemistry. Conversely, the adjacent regions would be rich in tungsten which would deposit on the walls. This non-uniform spot-blackening is indeed observed in horizontal lamps. Elimination of the stagnant region and the ensuing nonuniformity in tungsten distribution should therefore minimize blackening.

To this end, simulations of a modified lamp are performed. This lamp is distinguished by a deep 'vee' intrusion in the top region of the wall. The geometry and 29×29 computational grid are shown in Fig. 14. The velocity field and velocity contours (Figs. 15–17) show that the stagnant region is essentially eliminated by the turning guidance provided by the vee. Tungsten mass-fraction contours are shown in Fig. 18. These contours also show that the flow in the rest of the lamp remains unaffected by the geometrical modification suggested here. Because the

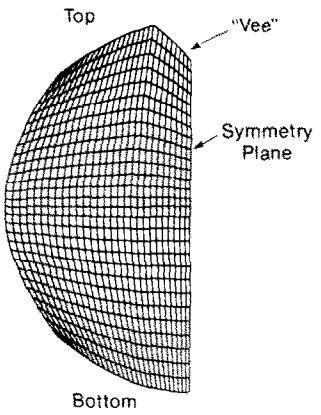

FIG. 14. Grid for a modified horizontal lamp.

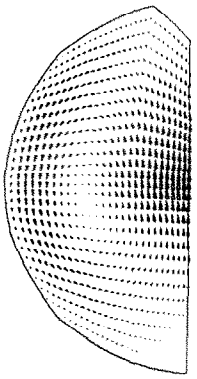

FIG. 15. Velocity field in a modified horizontal lamp.

flow at the bottom of the lamp is not influential, a similar vee could be introduced there making the lamp performance insensitive to a 180° rotation. Rather than the vee, cusped intrusions in the original circular envelope would serve the same purpose. The objective is to provide a continuous turning guidance which would retard flow separation and increase the velocities in the stagnant regions. The increased velocities enhance transport of all species by overwhelming differential diffusion; thus a more uniform distribution of all species and a reduced tendency to spot-blackening should result.

Figure 19 shows the convergence history of the simulations of the two horizontal lamps in terms of the mean kinetic energy, W, which was defined in equation (6). Convergence is attained when the curves asymptote to a horizontal line, indicating a steady state has been reached in the iterative solution process. The modified lamp is characterized by a larger kinetic energy, in part because the geometrical change in envelope shape guides the flow without the formation of a stagnation region at the top.

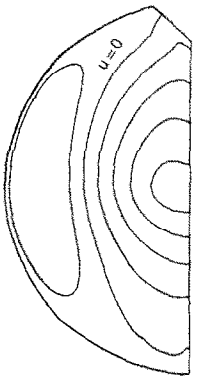

FIG. 16. Vertical velocity contours in a modified horizontal lamp ($\Delta u = 0.02\ \mathrm{m\,s^{-1}}$).

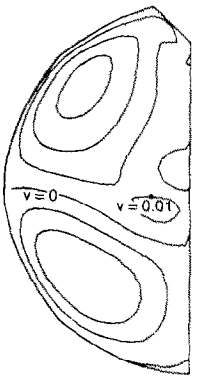

FIG. 17. Horizontal velocity contours in a modified horizontal lamp ($\Delta v = 0.01\mathrm{m\,s^{-1}}$).

5. CONCLUSIONS

The fluid flow and heat transfer in typical high-pressure incandescent lamps can be predicted using numerical solutions of the continuity, Navier–Stokes and energy equations. Vertically-oriented lamps are characterized by a boundary layer along the filament and a pronounced one-dimensional variation of temperature, with lateral displacement of isotherms only at the top and bottom of the lamp. Axial velocities just outside the boundary layer are of the order of $0.20\,\mathrm{m\,s^{-1}}$ with lower downward return velocities along the walls. Heat transfer so predicted from first principles agrees to within 15% with the semi-empirical Langmuir sheath theory. As a further check, with adiabatic end walls the variation of local heat transfer with height agrees with the functional behavior suggested by free convection theory.

In the horizontal case, the flow is dominated by a buoyant plume and stagnant region at the top of the lamp. A plausible mechanism linking this stagnant region to observed blackening patterns can be advanced. By understanding the fluid-mechanical basis of the stagnant region, a modified lamp geometry can be suggested. Computations show that this new lamp should indeed minimize the stagnant region and so, perhaps, the propensity for spot-blackening.

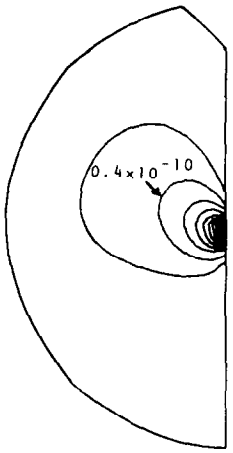

FIG. 18. Tungsten distribution in a modified horizontal lamp. Y_w.

The flow of tungsten vapor in these lamps resembles that of heat, as expected, since there are no sources or sinks for either quantity in the flow. Steep radial gradients at the filament confirm the presence of a boundary layer. Estimates of the life of the filament from the diffusional flux out of the filament are of the same order of magnitude as suggested by operational experience. In halogen lamps, the transport equation for inert tungsten flow would be replaced by a set for the minor species.

This study shows that computational models can be used to analyze the physical phenomena occurring in incandescent lamps. With these predicted velocity and temperature fields, a posteriori calculations of the dilute gas chemistry in halogen lamps may be performed.

REFERENCES

1. W. Elenbaas, The dissipation of heat by free convection from vertical and horizontal cylinders, *J. appl. Phys.* **19**, 1148 (1948).
2. I. Langmuir, Convection and conduction of heat in gases, *Phys. Rev.* **34**, 401 (1912).
3. F. J. Harvey, Mass transfer model of halogen doped incandescent lamps with application to the W-O-Br system, *Met. Transl. A* **7A**, 1167 (1976).
4. J. A. Sell, G. L. Easley and D. L. Simon, Laser Raman spectroscopy of tungsten halogen lamps, *Appl. Spectrosc.* **39**(1), 137 (1985).
5. G. De Vahl Davis and L. P. Jones, Natural convection in a square cavity: a comparison exercise, *Int. J. Num. Meth. Fluids* **3**, 227 (1983).
6. E. M. Sparrow and J. L. Gregg, Laminar free-convection heat transfer from the outer surface of a vertical circular cylinder, *Trans. Am. Soc. Mech. Engrs* 1823 (1956).
7. W. Shyy and S. M. Correa, A systematic comparison of several numerical schemes for complex flow calculations, AIAA Paper No. 85-0440 (1985).
8. S. V. Patankar and D. B. Spalding, A calculation procedure for heat, mass and momentum transfer in three-dimensional parabolic flows, *Int. J. Heat Mass Transfer* **15**, 1787 (1972).
9. W. Elenbaas, Rate of evaporation and heat dissipation of a heated filament in a gaseous atmosphere, *Philips Res. Rep.* **18**, 147 (1963).
10. R. B. Bergman, Private communications (1984).
11. W. H. McAdams, *Heat Transmission*, 3rd edn. McGraw-Hill, New York (1954).
12. J. M. Holeman, Visualization of gas convection in a lamp, General Electric Class III TIS Report (1973).
13. E. Fischer, J. Fitzgerald and H. Horster, Heat and mass transfer in gas-filled incandescent lamps, *J. IES* 271 (1975).

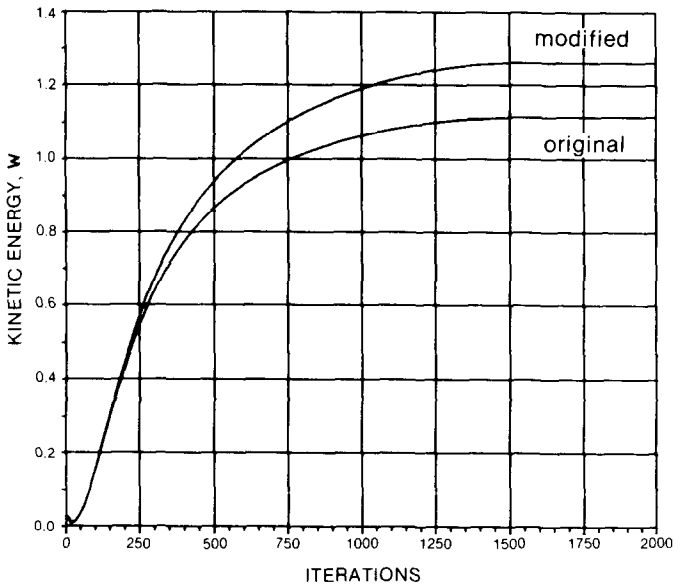

FIG. 19. Convergence histories of horizontal lamps.

MOUVEMENT DE FLUIDE ET TRANSFERT DE CHALEUR DANS LES LAMPES A INCANDESCENCE

Résumé—On développe un modèle numérique pour étudier la convection naturelle laminaire, bidimensionnelle, dans les lampes à incandescence avec une résolution par volume fini des équations de continuité, de Navier–Stokes et d'énergie sur une grille curvilinéaire. Le modèle est appliqué aux lampes orientées verticalement et horizontalement et contenant un gaz inerte à forte pression. Le transfert thermique du filament ainsi calculé s'accorde à 15% près avec une formule semi-empirique. Le transport des espèces diluées est formulé et calculé pour des vapeurs inertes de tungstène.

STRÖMUNG UND WÄRMEÜBERTRAGUNG IN GLÜHLAMPEN

Zusammenfassung—Es wird ein numerisches Modell zur Untersuchung der laminaren zweidimensionalen natürlichen Konvektionsströmung in Glühlampen entwickelt, worin die stationären Kontinuitäts-, Navier–Stokes- und Energiegleichungen mit Hilfe finiter Volumen in einem form-angepaßten Gitter gelöst werden. Das Modell wird auf typische, senkrecht und waagerecht orientierte Lampen, die ein hoch verdichtetes Inertgas enthalten, angewandt. Der berechnete Wärmeübergang am Glühfaden weicht weniger als 15% von einer halbempirischen Korrelation ab. Der Zusammenhang des Strömungsfeldes mit beobachteten geschwärzten Modellen wird diskutiert.

ТЕПЛОМАССОПЕРЕНОС ВНУТРИ ЛАМП НАКАЛИВАНИЯ

Аннотация—На основе стационарных уравнений неразрывности, Навье–Стокса и энергии с использованием метода конечного объема и соответствующей расчетной сетки построена численная модель двухмерной естественной конвекции внутри ламп накаливания. Конкретные расчеты выполнены для вертикально и горизонтально ориентированных ламп, содержащих инертный газ при высоком давлении. Предсказываемые характеристики теплопереноса от нити накала согласуются с известным полуэмпирическим соотношением с точностью до 15%. Обсуждается связь поля течений наблюдаемыми зонами потемнения. Сформулирована и решена задача о движении мелких частиц вольфрама в инертной атмосфере.